ISSN 1070-3284, Russian Journal of Coordination Chemistry, 2016, Vol. 42, No. 3, pp. 196–200. © Pleiades Publishing, Ltd., 2016.
Original Russian Text © P.A. Petrov, M.R. Ryzhikov, N.V. Kuratieva, S.N. Konchenko, 2016, published in Koordinatsionnaya Khimiya, 2016, Vol. 42, No. 3, pp. 173–177.

Cluster $[Re_3S_5(Dppe)_3]^+$ and Its Oxidation to $[Re_3S_4(SO_2)(Dppe)_3]^+$

P. A. Petrov[a, b, *], **M. R. Ryzhikov**[a, b], **N. V. Kuratieva**[a, b], **and S. N. Konchenko**[a, b]
[a] *Nikolaev Institute of Inorganic Chemistry, Siberian Branch, Russian Academy of Sciences,*
pr. akademika Lavrentieva 3, Novosibirsk, 630090 Russia
[b] *Novosibirsk State University, ul. Pirogova 2, Novosibirsk, 630090 Russia*
**e-mail: panah@niic.nsc.ru*

Received June 2, 2015

Abstract—The reaction of cluster $[Re_3S_4(Dppe)_3Br_3]Br$ with sodium *tert*-butyl thiolate affords trinuclear cationic cluster $[Re_3S_5(Dppe)_3]Br$ (**I**). The oxidation of cluster **I** with air gives $[Re_3S_4(SO_2)(Dppe)_3]Cl$ (**II**), which is characterized by X-ray diffraction analysis in the form of solvate **II** · $3.5CH_2Cl_2$ (CIF file CCDC 1401732). The DFT calculations indicate the triplet ground state of the $[Re_3S_5(Dppe)_3]^+$ cation and a significant spin density on the equatorial sulfide ligands, favoring the oxidation of the cluster.

DOI: 10.1134/S1070328416020056

INTRODUCTION

The chemistry of trinuclear chalcogenide rhenium clusters is poorly studied as compared to similar molybdenum and tungsten clusters and rhenium clusters of higher nuclearity [1]. Examples of these compounds are almost restricted by rhenium(V) chalcohalides containing the cluster core $[Re_3(\mu_3\text{-}Q)(\mu\text{-}Q_2)_3X_6]^+$ (Q = S, Se; Hal = Cl, Br) [2–5] and by products of their reactions with phosphines [6–10]. In addition, there are several examples of heterometallic complexes with the cluster core $\{Re_3M'(\mu_3\text{-}S)_4\}$ (M' = Ni, Co, Cu) [11–13].

We have recently synthesized complex $[Re_3S_4(Dppe)_3Br_3]Br$ (**III**) having nine cluster skeletal electrons and being the first example for the cluster core $\{Re_3S_4\}^{4+}$ coordinated by diphosphine ligands [14]. The structure of cation $[Re_3S_4(Dppe)_3Br_3]^+$ is nearly identical to the structure of its six-electron analog $[Mo_3S_4(Dppe)_3Br_3]^+$. Three additional electrons are localized on the Re atoms (as shown by the quantum-chemical calculations and EPR data) and exert no noticeable effect on the geometry of the cluster core. The synthesis of a complex with this stoichiometry makes it possible to study its reactions on the basis of the well studied chemistry of the molybdenum and tungsten analogs and to establish the influence of additional electrons of the rhenium atom on the chemical and electronic properties of the reaction products. We showed that the substitution of bromide ions in cluster $[Re_3S_4(Dppe)_3Br_3]^+$ by thiocyanate ions occurred with the retention of the high-spin ($S = 3/2$) state of the cluster core [15].

We also determined that the reaction of $[Mo_3S_4(Dppe)_3Br_3]PF_6$ with excess *tert*-BuSNa resulted in the rearrangement of the initial cluster core $\{Mo_3(\mu_3\text{-}S)(\mu\text{-}S)_3\}$ to more rare $\{Mo_3(\mu_3\text{-}S)_2(\mu\text{-}S)_3\}$ with two μ_3-bridging sulfide ligands and in the formation of the paramagnetic complex $[Mo_3S_5(Dppe)_3]PF_6$ [16].

This work is devoted to the synthesis of the rhenium analog of the discussed compound.

EXPERIMENTAL

The syntheses were carried out in an inert atmosphere using the standard Schlenk apparatus. Solvents for the syntheses were dehydrated and degassed by reflux and distillation in an inert gas using the corresponding drying agents [17]. The starting complex $[Re_3S_4(Dppe)_3Br_3]Br$ [14] was synthesized according to a known procedure. The IR spectra of the substances in KBr pellets were recorded on a SCIMITAR FTS 2000 instrument.

Synthesis of complex $[Re_3S_5(Dppe)_3]Br$ (I). A mixture of $[Re_3S_4(Dppe)_3Br_3]Br$ (177 mg, 0.080 mmol) and sodium *tert*-butyl thiolate (52 mg, 0.463 mmol) was placed in a Schlenk flask, and THF (25 mL) was added to the mixture. The obtained suspension was refluxed for 24 h, cooled, filtered through a glass filter (G4) with Celite, and evaporated. A dark residue was extracted with CH_2Cl_2 (~10 mL), and the extract was filtered through a glass filter (G4). The slow diffusion of Et_2O into the obtained solution resulted in the for-

Table 1. Crystallographic data and refinement parameters for structure **II** · $3.5CH_2Cl_2$

Parameter	Value
Empirical formula	$C_{81.5}H_{79}O_2P_6S_5Cl_8Re_3$
FW	2278.77
Crystal system; space group	Triclinic; *P*1
Temperature, K	150
a, Å	13.8639(5)
b, Å	13.8914(4)
c, Å	14.1867(5)
α, deg	65.973(1)
β, deg	86.467(1)
γ, deg	62.354(1)
V, Å^3	2183.03(13)
Z	1
F(000)	1115
μ, mm^{-1}	4.668
Crystal size, mm	0.46 × 0.14 × 0.06
T_{min}, T_{max}	0.223, 0.767
Data collection for θ range, deg	1.68–28.30
Range of indices *h*, *k*, *l*	$-17 \leqslant h \leqslant 18$, $-9 \leqslant k \leqslant 17$, $-17 \leqslant l \leqslant 18$
Number of measured/observed ($I > 2\sigma(I)$) reflections	17253/15354/14311
R_{int}	0.0198
R_1, wR_2 ($I > 2\sigma(I)$)	0.0256, 0.0622
R_1, wR_2 (all reflections)	0.0292, 0.0637
Goodness-of-fit	0.755
Number of refined parameters	959
Number of restraints	3
$\Delta\rho_{max}/\Delta\rho_{min}$, *e* Å^{-3}	1.75/–1.47

mation of a black powder of complex **I**. The yield was 25 mg (15%).

For $C_{78}H_{72}P_6S_5BrRe_3$

anal. calcd., %:	C, 46.98;	H, 3.64.
Found, %:	C, 46.30;	H, 3.70.

IR (KBr), cm^{-1}: 1585, 1572, 1484, 1434, 1414, 1335, 1311, 1276, 1191, 1159, 1123, 1097, 1027, 998, 906, 833, 741, 691, 617, 557. (+)-ES-MS (THF), *m*/*z*: 1913.12 ($[Re_3S_5(Dppe)_3]^+$, 100%).

X-ray diffraction analysis. Dark red crystals of compound **II** · $3.5CH_2Cl_2$ suitable for X-ray diffraction analysis were obtained by the slow diffusion of Et_2O into a solution of **I** in CH_2Cl_2 with air getting into the reaction mixture. The crystallographic and X-ray diffraction data for structure determination were obtained on a Bruker X8 Apex CCD automatic diffractometer (graphite monochromator, $\lambda(MoK_\alpha)$ = 0.71073 Å). An absorption correction was applied semiempirically using the SADABS program [18]. The structure was solved by the direct methods and refined by the least-squares method in the anisotropic approximation using the SHELXTL program package [18]. Hydrogen atoms were localized geometrically and refined in the rigid body approximation.

Table 2. Main parameters of the coordination nodes and chelate cycles in cluster **II** and its analogs

Compound	M—M	M–(μ_3-S)	M–(μ-X)
II	2.68 [3]	2.392 [14]	2.36 [3] (μ-S) 2.38 [4] (μ-SO_2)
IV	2.671 [13]	2.416 [16]	2.38 [2] (μ-S)
Im	2.719 [1]	2.450 [6]	2.428 [7]
IIm	2.74 [4]	2.456 [14]	2.388 [13] (μ-S) 2.461 [2] (μ-SO_2)
IVm	2.725 [5]	2.492 [2]	2.438 [10]

The crystallographic data and refinement parameters for the structure are presented in Table 1. Selected bond lengths and angles are given in Table 2. The coordinates of atoms were deposited with the Cambridge Crystallographic Data Centre (CIF file CCDC 1401732; deposit@ccdc.cam.ac.uk or http://www.ccdc.cam.ac.uk/data_request/cif) and are available from the authors.

Quantum-chemical calculations using the density functional theory (DFT) were performed in the ADF2012 program package [19, 20]. Geometry optimization was carried out with the VWN+BP86 density functional [21–24] and the TZP incomplete-electron Slater-type basis set [25] in which only electrons Re.5*s*5*p*5*d*6*s*, Mo.4*d*5*s*, S.3*s*3*p*, P.3*s*3*p*, O.2*s*2*p*, C.2*s*2*p*, and H.1*s* were varied. The rest electrons were considered in the frozen core approximation [19]. Scalar relativistic effects were taken into account by the ZORA method [26]. To simplify the calculations, the peripheral phenyl groups of the Dppe ligand were replaced by methyl groups. The optimized structures have no imaginary frequencies, indicating that the system is in the local energy minimum. The energy of formation was calculated relatively to the energy of spherically symmetrical atoms calculated in the spin-restricted approximation. For the characterization of the electronic structure, we used calculations at the point with the coordinates of atoms obtained by the geometry optimization procedure using the VWN+BP86 functional and the TZP all-electron basis set. The spin density was constructed in the DGrid program [27] of the wave functions obtained in the all-electron basis set. Integration over the atom basin determined in the framework of the QTAIM method [28] was used to obtain spin densities for atoms.

RESULTS AND DISCUSSION

The reaction of sodium *tert*-butyl thiolate and *nido*-cubane cluster **III** leads, as in the case of the molybdenum analog, to the transformation of the starting cluster core $\{Re_3(\mu_3\text{-}S)(\mu\text{-}S)_3\}$ into the earlier unknown $\{Re_3(\mu_3\text{-}S)_2(\mu\text{-}S)_3\}$ cluster and to the formation of complex **I**.

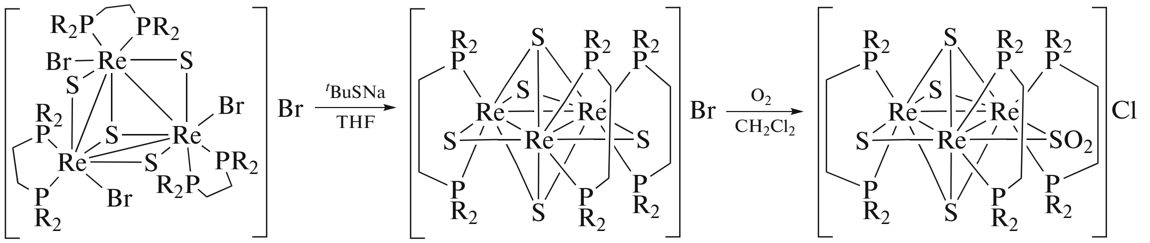

III (R = Ph) **I** (R = Ph) **Im** (R = Me) **II** (R = Ph) **IIm** (R = Me)

Evidently, *tert*-BuSNa is the reducing agent and a source of the additional S atom. The main distinction from the molybdenum analog is the tendency of cluster **I** to oxidation, which did not allow its isolation as single crystals suitable for X-ray diffraction analysis. In spite of this, mass spectrometry showed that a solution of complex **I** contains the single set of signals in the range *m/z* 1000–2500 corresponding to cation $[Re_3S_5(Dppe)_3]^+$ (*m/z* 1913.12).

An attempt to crystallize complex **I** by diethyl ether diffusion into a solution in CH_2Cl_2 gave several red crystals. According to the X-ray diffraction data, the isolated complex has the composition $[Re_3S_5O_2(Dppe)_3]Cl \cdot 3.5CH_2Cl_2$ (**II** · $3.5CH_2Cl_2$) and represents the product of the addition of dioxygen to one of the equatorial sulfide ligands due to a minor amount of air that got into the reaction mixture (Fig. 1). This behavior is typical of the triangular rhenium sulfide complexes and is not typical of their molybdenum and tungsten analogs. Rhenium clusters, viz., the addition products of dioxygen with the composition $[Re_3S_3(SO_2)Cl_6(Phos)_3]^-$ (Phos = PEt_3 [8], PMe_2Ph [9]), were isolated earlier and characterized by X-ray diffraction analysis. As in the case of compound **I**, it is the μ_2-bridged sulfide which is oxidized. An impurity of $[Re_3S_4O_2(Dppe)_3Br_3]^+$ was observed by mass spectrometry in a solution of $[Re_3S_4(Dppe)_3Br_3]^+$. Mixed-halide clusters $[Re_3S_4(Dppe)_3Br_xCl_{3-x}]^+$ are oxidized to $[Re_3S_4O_2(Dppe)_3Br_xCl_{3-x}]^+$ [14]. Tetranuclear cluster $[Re_4(\mu_3\text{-}S)_2(\mu\text{-}SO_2)_4(CN)_{10}]^{8-}$ [29] is also the oxidation product of all μ_2-bridged sulfides, whereas the μ_3-sulfide ligands do not undergo oxidation.

Complex **II** crystallizes in the form of solvate (1 : 3.5) with CH_2Cl_2 molecules. The $\{Re_3S_5\}$ skeleton has a shape of somewhat distorted trigonal bipyramid. Each face of the triangle Re_3 is coordinated by two μ-S and one μ-SO_2 ligand. The Re(2)–Re(3) distance is 2.6427(5) Å, which corresponds to the bond at μ-SO_2 and is somewhat shorter than two other rhenium–rhenium bonds (2.6950(3) and 2.7008(3) Å). The S(3) and S(4) atoms lie almost in the Re(1)Re(2)Re(3) plane, whereas S(5) deviates sig-

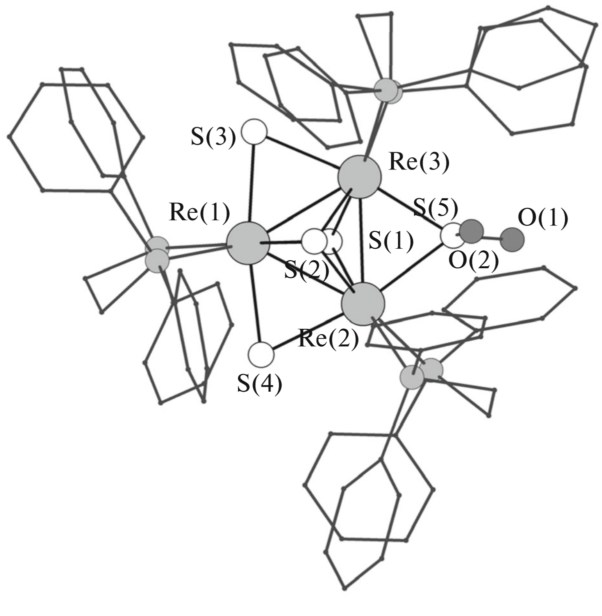

Fig. 1. Structure of the cation in complex **II**. Hydrogen atoms are omitted. Selected bond lengths (Å): Re(1)–Re(2) 2.7008(3), Re(1)–Re(3) 2.6950(3), Re(2)–Re(3) 2.6432(3), S(5)–O(1) 1.481(5), and S(5)–O(2) 1.494(4).

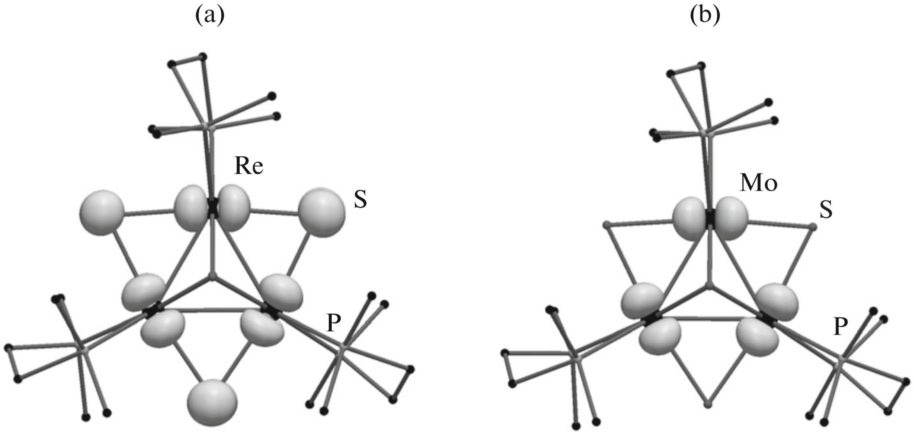

Fig. 2. Structures and spin density isosurfaces of clusters (a) **Im** and (b) **IVm** (the spin density isosurface is equal to –0.01 au).

nificantly (by 0.38 Å) from this plane. The S–O distances (1.481(5) and 1.494(4) Å) are somewhat longer than those in $[Re_3S_4O_2Cl_6(PEt_3)_3]^-$ and $[Re_3S_4O_2Cl_6(PMe_2Ph)_3]^-$, and the O(1)S(5)O(2) angle is 110.1(3)°. The chloride ion formed, most likely, in situ from CH_2Cl_2 acts as a counterion, which is an additional factor decreasing the yield of complex **II**.

The average Re–Re bond length in cluster **II** (2.68 [3] Å) is close to that in the ten-electron complex $[Re_3S_4(PEt_3)_4Br_3]$ (2.67 [2] Å) [6]. The Mo–Mo distances in the seven-electron cluster $[Mo_3S_5(Dppe)_3]^+$ **(IV)**, having the same average oxidation state of the metal (+3.67), are also similar. However, it should be mentioned that the transformation of the cluster core $\{Re_3S_4\}$ into $\{Re_3S_3(SO_2)\}$ results in the elongation of the Re–Re bonds by ~0.08 Å [8, 9].

In order to explain reasons for the fast oxidation of cluster Re_3S_5, we performed the quantum-chemical calculations of model clusters $[Re_3S_5(Dmpe)_3]^+$ **(Im)** and $[Re_3S_5O_2(Dmpe)_3]^+$ **(IIm)**, which differ from **I** and **II** by the replacement of all phenyl groups by methyl groups. The interatomic distances calculated for cluster **IIm** are consistent with the experimental bond lengths in complex **II** (Table 2). The energies of formation of the clusters are presented in Table 3. It is seen that the triplet state is more favorable for the cluster with the Re_3S_5 core (the cluster with $S = 0$ is by 6.4 kcal/mol less stable than the cluster with $S = 1$). On the contrary, the closed shell is preferential for the cluster with the oxidized core $Re_3S_5O_2$ (the cluster with $S = 0$ is by 12.9 kcal/mol more stable than the cluster with $S = 1$). The calculations also showed a significant spin density on the equatorial sulfur atoms of complex **Im** (Fig. 2a, Table 4), which seems to favor the interaction of the complex with air oxygen. The spin density distribution in a similar molybdenum cluster $[Mo_3S_5(Dmpe)_3]^+$ **(IVm)** with one unpaired electron was calculated for comparison. It was found that the spin density on the sulfur atoms in complex **IVm** is almost absent. Possibly, the spin density on the bridging sulfide ligands facilitates the interaction with oxygen. In this case, the diamagnetic cluster with the $Re_3S_5O_2$ core ($S = 0$) should not add extra oxygen molecules, which is experimentally observed.

Table 3. Energies of formation (kcal/mol) for the cluster cations in different spin states

Compound	$S = 0$	$S = 1$
$[Re_3S_5(Dmpe)_3]^+$ **(Im)**	–9621.12	–9627.51
$[Re_3S_5O_2(Dmpe)_3]^+$ **(IIm)**	–9917.28	–9904.35

Table 4. Calculated spin density (minimum/maximum) on the atoms of the cluster core $\{M_3S_5\}$

Atom	$[Re_3S_5(Dmpe)_3]^+$ **(Im)**	$[Mo_3S_5(Dmpe)_3]^+$ **(IVm)**
M	0.34/0.35	0.38/0.40
μ_3-S	0.00	–0.01
μ-S	0.31/0.28	–0.07/–0.05

Thus, the first example of the cluster with the $\{Re_3S_5\}$ core was obtained. The product of dioxygen addition to this cluster was characterized by X-ray diffraction analysis and quantum-chemical calculations.

ACKNOWLEDGMENTS

The authors are grateful to M. Neumaier (Karlsruhe Institute of Technology, Germany) for the registration of mass spectra.

This work was supported by the Russian Science Foundation, project no. 14-23-000-13.

REFERENCES

1. Saito, T., *J. Chem. Soc., Dalton Trans.*, 1999, p. 97.
2. Timoshchenko, N.I., Kolesnichenko, V.L., Volkov, S.V., et al., *Koord. Khim.*, 1990, vol. 16, no. 8, p. 1062.

3. Beck, J. and Müller-Buschbaum, K., *Z. Anorg. Allg. Chem.*, 1999, vol. 625, p. 1212.
4. Rybakov, V.B., Yanko, O.G., Aslanov, L.A., et al., *Russ. J. Coord. Chem.*, 2000, vol. 26, no. 7, p. 482.
5. Volkov, S.V., Fokina, Z.A., Yanko, O.G., et al., *Russ. J. Inorg. Chem.*, 2005, vol. 50, no. 8, p. 1150.
6. Yamada, S., Miyake, N., Imoto, H., and Saito, T., *Chem. Lett.*, 1997, vol. 26, p. 671.
7. Miyake, N., Imoto, H., and Saito, T., *Chem. Lett.*, 1997, vol. 26, p. 913.
8. Sokolov, M., Imoto, H., and Saito, T., *Chem. Lett.*, 1998, vol. 27, p. 949.
9. Saito, T., Sunaga, T., Sakai, N., et al., *Inorg. Chem.*, 2005, vol. 44, p. 4427.
10. Petrov, P.A., Peresypkina, E.V., Virovets, A.V., et al., *J. Struct. Chem.*, 2006, vol. 47, no. 5, p. 985.
11. Miyake, N., Imoto, H., and Saito, T., *Chem. Lett.*, 1997, vol. 26, p. 631.
12. Sakai, N. and Saito, T., *Polyhedron*, 2004, vol. 23, p. 2611.
13. Iijima, K., Sunaga, T., Hirose, M., and Saito, T., *Inorg. Chem.*, 2006, vol. 45, p. 3452.
14. Petrov, P.A., Virovets, A.V., Bogomyakov, A.S., et al., *Chem. Commun.*, 2012, vol. 48, p. 2713.
15. Petrov, P.A., Afonin, M.Yu., Naumov, D.Yu., et al., *Russ. J. Coord. Chem.*, 2014, vol. 40, no. 4, p. 200.
16. Petrov, P.A., Virovets, A.V., Alberola, A., et al., *Dalton Trans.*, 2010, vol. 39, p. 8875.
17. Gordon, A. and Ford, R., *The Chemist's Companion: A Handbook of Practical Data, Techniques, and References*, New York: Wiley, 1972.
18. *APEX2 (version 1.08), SAINT (version 7.03), SADABS (version 2.11), SHELXTL (version 6.12)*, Madison: Bruker AXS Inc., 2004.
19. Velde, G. te, Bickelhaupt, F.M., van Gisbergen, S.J.A., et al., *J. Comput. Chem.*, 2001, vol. 22, p. 931.
20. *ADF2014. SCM. Theoretical Chemistry*, Amsterdam: Vrije Univ., 2014. http://www.scm.com
21. Vosko, S.H., Wilk, L., and Nusair, M., *Can. J. Phys.*, 1980, vol. 58, p. 1200.
22. Becke, A.D., *Phys. Rev. A: At., Mol., Opt. Phys.*, 1988, vol. 38, p. 3098.
23. Perdew, J.P., *Phys. Rev. B: Condens. Mater. Mater. Phys.*, 1986, vol. 33, p. 8822.
24. Perdew, J.P., *Phys. Rev. B: Condens. Mater. Mater. Phys.*, 1986, vol. 34, p. 7406.
25. van Lenthe, E. and Baerends, E.J., *J. Comput. Chem.*, 2003, vol. 24, p. 1142.
26. van Lenthe, E., Ehlers, A.E., and Baerends, E.J., *J. Chem. Phys.*, 1999, vol. 110, p. 8943.
27. Kohout, M., *DGrid (version 4.6)*, Radebeul, 2011.
28. Bader, R., *Atoms in Molecules. A Quantum Theory*, New York: Oxford Univ., 1990.
29. Müller, A., Krickemeyer, E., Bögge, H., et al., *Angew. Chem., Int. Ed. Engl.*, 1994, vol. 33, p. 770.

Translated by E. Yablonskaya